

DYNAMIC RECRYSTALLIZATION OF A QUARTZ PORPHYROCLAST

G. E. Lloyd,
Department of Earth Sciences, The University,
Leeds LS2 9JT, England.

B. Freeman,
Badley, Ashton and Associates, Winceby House,
Winceby, Lincolnshire LN9 6PB, England.

Dynamic recrystallization occurs to minimize strain energy via either grain boundary migration or subgrain rotation^{1,2}. Both result in similar microstructures, but whereas in the former new grains have their crystallographic orientation controlled by neighbouring grains, in the latter new grains are derived from the parent grain. We have used the scanning electron microscope (SEM) electron channelling (EC) technique³⁻⁷ and the program CHANNEL⁸ to distinguish the contribution of these processes in a 50% recrystallized quartz porphyroclast (Crinan Grits, Dalradian, SW Highlands, Scotland; 370-400°C)^{9,10}. This grain exhibits a core region of subgrains and a mantle region of neoblast grains (Fig. 1).

SEM/EC OBSERVATIONS

We have obtained ECP's from 52 subgrain and neoblast regions (Fig. 1) and derived from them crystal axes pole figures (Fig. 2). The subgrains are represented by clusters which define a "single crystal" orientation typical of the original porphyroclast. Neoblast grains generally have large misorientations relative to the original orientation. Nevertheless, we have been able to recognize several orientation relationships (Table 1) which depict the dispersion trails away from the porphyroclast orientation. This suggests that dynamic recrystallization occurred via rotational

processes, with the original orientation of the porphyroclast defining the positions of the potential rotation axes (C, M1-3, A1-3 etc.) for specific crystal slip systems (Fig. 2). We must now identify the slip systems involved.

Table 1. Relationships (B) between porphyroclast (P), core subgrains (S) and mantle neoblasts (N) crystal axes: *, coincident; +, slight dispersion; b, dispersion in porphyroclast basal plane.

No.	GRP	CRYSTAL AXES						No.	GRP	CRYSTAL AXES					
		C ==M==			==A==					C ==M==			==A==		
		1	2	3	1	2	3			1	2	3	1	2	3
N01	B3	*	b	b	b	b	b	N31	B1b						+
N02	B1a			*				S32		*	*	*	*	*	*
N03	B3	*	b	b	b	b	b	S33		*	*	*	*	*	*
N04	B3	+	b	b	b	b	b	S34		*	*	*	*	*	*
N07	B3	+	b	b	b	b	b	S35		*	*	*	*	*	*
N10	B3	+	b	b	b	b	b	S36		*	*	*	*	*	*
N11	B3	+	b	b	b	b	b	S37		*	*	*	*	*	*
N12	B3	+	b	b	b	b	b	S38		P	P	P	P	P	P
N13	B1a				+			S39		*	*	*	*	*	*
N14	B1b						*	S40		*	*	*	*	*	*
N15	B1b						*	S41		*	*	*	*	*	*
N16	B1a			+				S42		*	*	*	*	*	*
N17	B1b						*	S43		*	*	*	*	*	*
N18	B1a		*				+	S44		*	*	*	*	*	*
N19	B4							S45		*	*	*	*	*	*
N20	B4							S46		*	*	*	*	*	*
N21	B4							S47		*	*	*	*	*	*
N22	B1b	+	+	+	+	*	+	N48	B1a		+				
N23	B4							N49	B1b					+	
N24	B4							N50	B1a		*				
N25	B4							N51	B2	*	*	*	*	*	*
N26	B2	*	*	*	*	*	*	N52	B1a		+				
N27	B2	*	*	*	*	*	*	N53	B1a		*				
N28	B1b						*	N54	B1a		+				
N29	B1a					*		N55	B1a		*				
N30	B4							N56	B2	*	*	*	*	*	*

CRYSTAL SLIP SYSTEMS

To illustrate the dispersion paths for the small numbers of data involved, we have derived¹¹

pole figures (Figs. 3) from the true orientation distribution function (ODF) calculated from the discrete ECP data. The subgrain pole figures (Fig. 3b) show slight, bidirectional dispersions. The M1 cluster has the minimum dispersion, whilst the C-A3 elliptical clusters are elongate within their common great circle. These observations are consistent with subgrain polygonization accommodated by A3 basal-a slip centred on M1.

The crystal textures of neoblasts show complex dispersion patterns (Fig. 3c). However, we have seen that distinct groups can be recognized (Table 1). We have therefore divided the neoblast data into these groups and derived pole figures (Fig. 4) from their true ODF's.

Group B1a (Fig. 4a): M1 cluster; M2-M3 and A1-A2 small circles; and C-A3 great circle. This is consistent with A3 basal-a slip centred on M1. Group B1b (Fig. 4b): a cluster slightly displaced from A3; A1-A2 and M2-M3 small circles; and C-M1 great circle. This is consistent with M1 basal-m slip centred on a displaced A3. The displacement of the a cluster occurs on the great circle distribution produced by basal-a slip, which suggests that basal-m slip occurred after basal-a slip.

Group B2 neoblasts show (Fig. 4c) identical dispersion paths to the core subgrains (Fig. 3b), which suggests that they are original subgrains preserved within the mantle.

Group B3 (Fig. 4d): C cluster and a combined M1-3, A1-3 great circle. This is consistent with "basal-prism" slip centred on C, although we have been unable to determine the specific system.

Group B4 (Fig. 4e) neoblasts are significantly dispersed from the original orientations. However, clustering of certain axes suggests common dispersion paths exist but probably involving several slip systems. For example, consider the m-axis cluster represented by the "density maximum". This consists of neoblasts 19-21, but their complete orientations are different (Fig. 5a) and can be produced as

follows (Fig. 5b): 1. **A3 basal-a** slip centred on **M1**; 2. **M3 basal-m** slip centred on the modified **A2**; and 3. **A1 basal-a** slip centred on the doubly modified **M2**. The final step is responsible for the separation of the two neoblast orientations (except for the common **M2 m**-axis) because it operates in opposite (i.e. axial) directions.

Some neoblasts (4, 13, 16, 19, 20) do not share a common orientation (Fig. 5c) but are large relative to neoblasts which do share the same slip system characteristics. A simple explanation is that these neoblasts have undergone grain growth via grain boundary migration, probably at the expense of neighbouring neoblasts.

CONCLUSIONS

Our SEM/EC analyses suggest that the dynamic recrystallization of an individual quartz porphyroclast is a sequential process. Recrystallization initiates by subgrain polygonization on a single slip system. This develops into subgrain rotation. Continued rotation to achieve large misorientations requires more than one active slip system. However, this microstructure may be unstable and large "internal" strain energies may develop which are sufficient to initiate migration of grain boundaries.

REFERENCES

1. M.R. Drury, F.J. Humphreys and S.H. White, *Phys. Earth Planet. Interns.* **40**, 208-222 (1985).
2. J.L. Urai, W.D. Means and G.S. Lister, *Geophys. Monogr. Ser.* **36**, 161-199 (1986).
3. D.C. Joy, D.E. Newbury and D.L. Davidson, *J. Appld. Phys.* **53**, R81-R122 (1982).
4. G.E. Lloyd and C.C. Ferguson, *J. Struct. Geol.* **8**, 517-526 (1986).
5. G.E. Lloyd, *Mineral. Mag.* **51**, 3-19 (1987).
6. G.E. Lloyd, C.C. Ferguson and R.D. Law, *Tectonophysics* **135**, 243-249 (1987).
7. M.G. Hall and G.K. Skinner, *J. Phys. E*, **11**, 1129-1132 (1978).

8. N-H. Schmidt and N.O. Olesen, *Canad. Mineral*, **27**, 15-22 (1989).
9. B. Freeman, Unpubld. Ph.D. Thesis (Univ. of Nottingham, England, 1985).
10. B. Freeman, *J. Struct. Geol.* **6**, 655-662 (1984).
11. G.E. Lloyd, N-H. Schmidt, D. Mainprice, N.O. Olesen, R.D. Law, & M. Casey, *This Conference* (1990).

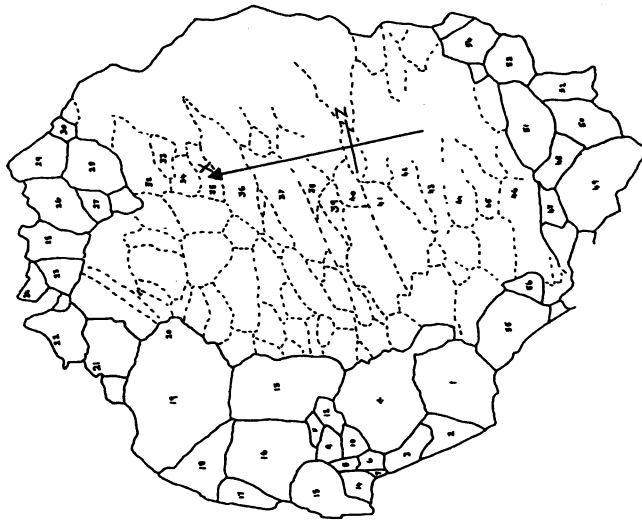


Figure 1. Quartz porphyroclast showing positions of core subgrains and mantle neoblasts.

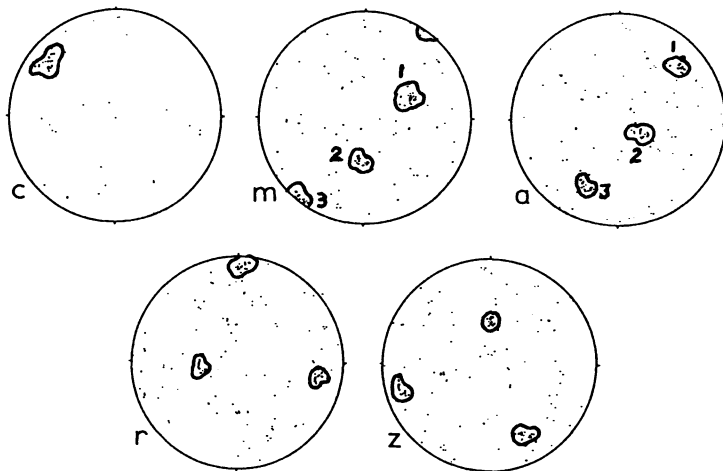


Figure 2. ECP/CHANNEL derived pole figures.

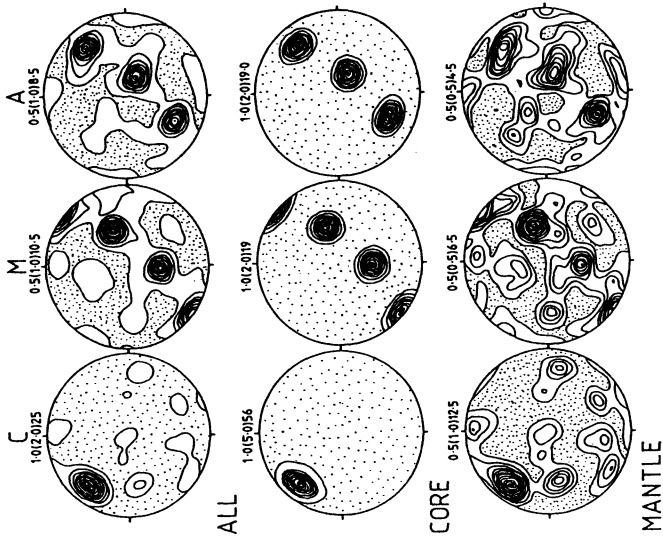


Figure 3. Pole figures derived from the true ODF.

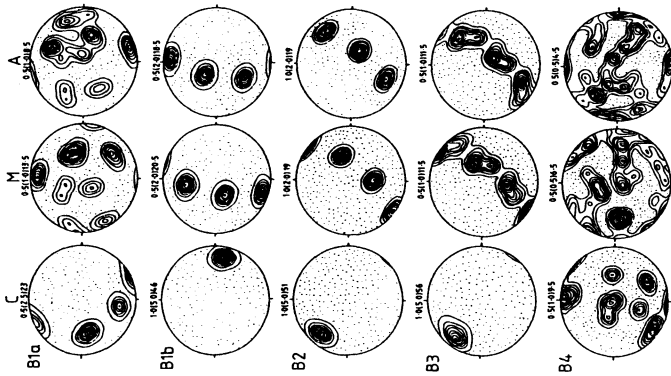


Figure 4. Mantle neoblast pole figures.

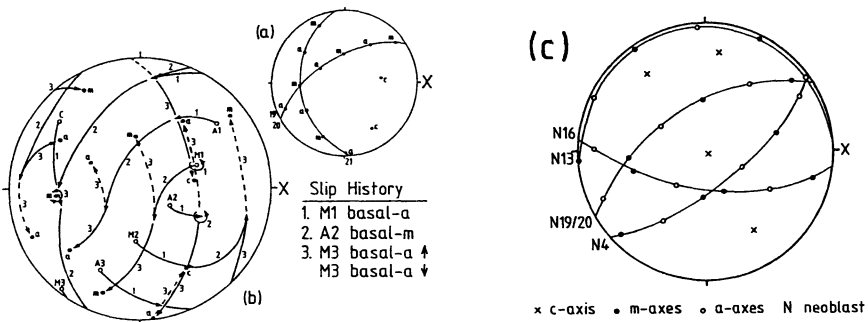


Figure 5. Examples of Group 4 neoblasts.